

Search for neutrinoless decays

$$\tau \rightarrow \ell h h \text{ and } \tau \rightarrow \ell V^0$$

Belle Collaboration

Y. Yusa^{ap}, K. Abe^f, K. Abe^{aj}, I. Adachi^f, H. Aihara^{al},
Y. Asano^{ao}, V. Aulchenko^a, A. Bay^{el}, U. Bitenc^j, I. Bizjak^j,
S. Blyth^r, A. Bondar^a, T. E. Browder^e, A. Chen^r,
B. G. Cheon^c, Y. Choi^{af}, Y. K. Choi^{af}, A. Chuvikov^{ab},
S. Cole^{ag}, J. Dalseno^o, M. Dash^{ap}, A. Drutskoy^d,
S. Eidelman^a, S. Fratina^j, N. Gabyshev^a, T. Gershon^f,
G. Gokhroo^{ah}, A. Gorišek^j, H. C. Ha^k, J. Haba^f,
K. Hayasaka^p, H. Hayashii^q, M. Hazumi^f, Y. Hoshi^{aj},
W.-S. Hou^s, T. Iijima^p, K. Ikado^p, K. Inami^p, R. Itoh^f,
M. Iwasaki^{al}, Y. Iwasaki^f, J. H. Kang^{aq}, H. Kawai^b,
T. Kawasaki^v, H. R. Khan^{am}, H. Kichimi^f, S. K. Kim^{ae},
S. Korpar^{n,j}, P. Križan^{m,j}, R. Kulasiri^d, C. C. Kuo^r,
A. Kuzmin^a, Y.-J. Kwon^{aq}, T. Lesiak^t, S.-W. Lin^s,
D. Liventsevⁱ, G. Majumder^{ah}, T. Matsumoto^{an}, W. Mitaroff^h,
Y. Miyazaki^p, R. Mizukⁱ, T. Nagamine^{ak}, E. Nakano^x,
Z. Natkaniec^t, S. Nishida^f, S. Ogawa^{ai}, T. Ohshima^p,
T. Okabe^p, S. L. Olsen^e, Y. Onuki^v, H. Ozaki^f, P. Pakhlovⁱ,
H. Palka^t, R. Pestotnik^j, L. E. Piilonen^{ap}, Y. Sakai^f, N. Sato^p,
T. Schietinger^{el}, O. Schneider^{el}, C. Schwanda^h, R. Seidl^{ac},
K. Senyo^p, M. Shapkin^g, H. Shibuya^{ai}, B. Shwartz^a,
A. Sokolov^g, A. Somov^d, N. Soni^z, R. Stamen^f, S. Stanič^w,
M. Starič^j, K. Sumisawa^y, O. Tajima^f, F. Takasaki^f,
K. Tamai^f, M. Tanaka^f, G. N. Taylor^o, Y. Teramoto^x,
X. C. Tian^{aa}, T. Tsukamoto^f, S. Uehara^f, S. Uno^f, Y. Usov^a,
G. Varner^e, S. Villa^{el}, E. Won^k, B. D. Yabsley^{ag},
A. Yamaguchi^{ak}, Y. Yamashita^u, M. Yamauchi^f and
Z. P. Zhang^{ad}

^a*Budker Institute of Nuclear Physics, Novosibirsk, Russia*

- ^b*Chiba University, Chiba, Japan*
- ^c*Chonnam National University, Kwangju, South Korea*
- ^d*University of Cincinnati, Cincinnati, OH, USA*
- ^e*University of Hawaii, Honolulu, HI, USA*
- ^f*High Energy Accelerator Research Organization (KEK), Tsukuba, Japan*
- ^g*Institute for High Energy Physics, Protvino, Russia*
- ^h*Institute of High Energy Physics, Vienna, Austria*
- ⁱ*Institute for Theoretical and Experimental Physics, Moscow, Russia*
- ^j*J. Stefan Institute, Ljubljana, Slovenia*
- ^k*Korea University, Seoul, South Korea*
- ^l*Swiss Federal Institute of Technology of Lausanne, EPFL, Lausanne, Switzerland*
- ^m*University of Ljubljana, Ljubljana, Slovenia*
- ⁿ*University of Maribor, Maribor, Slovenia*
- ^o*University of Melbourne, Victoria, Australia*
- ^p*Nagoya University, Nagoya, Japan*
- ^q*Nara Women's University, Nara, Japan*
- ^r*National Central University, Chung-li, Taiwan*
- ^s*Department of Physics, National Taiwan University, Taipei, Taiwan*
- ^t*H. Niewodniczanski Institute of Nuclear Physics, Krakow, Poland*
- ^u*Nippon Dental University, Niigata, Japan*
- ^v*Niigata University, Niigata, Japan*
- ^w*Nova Gorica Polytechnic, Nova Gorica, Slovenia*
- ^x*Osaka City University, Osaka, Japan*
- ^y*Osaka University, Osaka, Japan*
- ^z*Panjab University, Chandigarh, India*
- ^{aa}*Peking University, Beijing, PR China*
- ^{ab}*Princeton University, Princeton, NJ, USA*
- ^{ac}*RIKEN BNL Research Center, Brookhaven, NY, USA*
- ^{ad}*University of Science and Technology of China, Hefei, PR China*
- ^{ae}*Seoul National University, Seoul, South Korea*
- ^{af}*Sungkyunkwan University, Suwon, South Korea*
- ^{ag}*University of Sydney, Sydney, NSW, Australia*
- ^{ah}*Tata Institute of Fundamental Research, Bombay, India*
- ^{ai}*Toho University, Funabashi, Japan*
- ^{aj}*Tohoku Gakuin University, Tagajo, Japan*
- ^{ak}*Tohoku University, Sendai, Japan*

^{al}*Department of Physics, University of Tokyo, Tokyo, Japan*

^{am}*Tokyo Institute of Technology, Tokyo, Japan*

^{an}*Tokyo Metropolitan University, Tokyo, Japan*

^{ao}*University of Tsukuba, Tsukuba, Japan*

^{ap}*Virginia Polytechnic Institute and State University, Blacksburg, VA, USA*

^{aq}*Yonsei University, Seoul, South Korea*

Abstract

We have searched for neutrinoless τ lepton decays into ℓhh or ℓV^0 , where ℓ stands for an electron or muon, h for a charged light hadron, π or K , and V^0 for a neutral vector meson, ρ^0 , $K^*(892)^0$ and ϕ , using a 158 fb^{-1} data sample collected with the Belle detector at the KEKB e^+e^- collider. Since the number of events observed are consistent with the expected background, we set upper limits on the branching fractions in the range of $(1.6 - 8.0) \times 10^{-7}$ for various decay modes at the 90% confidence level.

Key words: TAU Lepton Flavor Violation

PACS: 11.30.-j, 12.60.-i, 13.35.Dx, 14.60.Fg

1 Introduction

In the Standard Model (SM), lepton-flavor-violating (LFV) decays of charged leptons are forbidden, or highly suppressed even if the effect of neutrino mixing is taken into account [1]. In contrast, LFV decay processes are expected to appear with much larger branching fractions than those in the SM if there are contributions from new physics. Searches for LFV decay processes may thus reveal new physics beyond the SM. Some models predict LFV decays of τ leptons at a level accessible at the high luminosity B -factories [2,3]. In this paper, we report on a search for LFV in fourteen τ^- decay modes into neutrinoless final states with one charged lepton ℓ and two charged pseudoscalar mesons h : $e^-\pi^+\pi^-$, $e^+\pi^-\pi^-$, $\mu^-\pi^+\pi^-$, $\mu^+\pi^-\pi^-$, $e^-\pi^+K^-$, $e^-\pi^-K^+$, $e^+\pi^-K^-$, $e^-K^+K^-$, $e^+K^-K^-$, $\mu^-\pi^+K^-$, $\mu^-\pi^-K^+$, $\mu^+\pi^-K^-$, $\mu^-K^+K^-$ and $\mu^+K^-K^-$, and eight modes in which τ decays into one lepton and one vector meson: $e^-\rho^0$, $e^-K^*(892)^0$, $e^-\bar{K}^*(892)^0$, $e^-\phi$, $\mu^-\rho^0$, $\mu^-K^*(892)^0$, $\mu^-\bar{K}^*(892)^0$ and $\mu^-\phi$.¹ Current upper bounds on the branching fractions for these decays are of the order of 10^{-6} at 90% confidence level (CL) and have been set in the CLEO experiment using a data sample of 4.79 fb^{-1} [4]. Very recently CLEO results on $\tau \rightarrow \ell hh$ modes were improved by the BaBar experiment and upper

¹ Charge conjugate decay modes are implied throughout the paper.

limits in the range $(0.7 - 4.8) \times 10^{-7}$ were obtained from a 221.4 fb^{-1} data sample [5]. We present here results of a new search based on a data sample of 158.0 fb^{-1} corresponding to 140.9×10^6 τ -pairs collected with the Belle detector [6] at the KEKB asymmetric-energy e^+e^- collider [7] operating at or near the $\Upsilon(4S)$ resonance.

2 Event Selection

The Belle detector is a general purpose detector with excellent capabilities for precise vertex determination and particle identification. Tracking of charged particles is performed using a three-layer double-sided silicon vertex detector (SVD) and a fifty-layer cylindrical drift chamber (CDC) located in a 1.5 T magnetic field. Charged hadrons are identified by combining dE/dx information from the CDC, signal pulse-heights from aerogel Čerenkov counters (ACC) and timing information from time-of-flight scintillation counters (TOF). Photons are reconstructed using a CsI(Tl) electromagnetic calorimeter (ECL). Muons are detected by fourteen layers of resistive plate counters interleaved with iron plates (KLM).

We use TAUOLA [8] for Monte Carlo (MC) event generation of τ -pair signals and KKMC [9] to implement initial and final state radiation. The KKMC MC program predicts a cross-section of $\sigma(e^+e^- \rightarrow \tau^+\tau^-) = (0.8916 \pm 0.0006) \text{ nb}$ at the center-of-mass energy of KEKB. We calculate the number of τ -pair events from the cross section and measured integrated luminosity $\mathcal{L}_{\text{int}} = 158.01 \text{ fb}^{-1}$. The MC data is processed through the Belle detector simulation program based on GEANT3 [10] to determine signal efficiencies. We use the CLEO QQ event generator [11] for hadronic events and AAFHB [12] for two-photon events, and study their contributions to the background of each τ decay mode.

We search for τ -pair events in which one τ decays into the ℓhh (3-prong) final state. The other τ dominantly decays into one charged particle and any number of neutrals (1-prong) with a branching fraction of 85.35% [13]. We require that there be four charged tracks with zero net charge and any number of photons in an event. We reconstruct the trajectory of a charged track from hits in the SVD and CDC, and require that a reconstructed transverse momentum be larger than $0.1 \text{ GeV}/c$ and polar angle θ be within the range $25^\circ < \theta < 140^\circ$, with respect to the direction opposite to the e^+ beam. For all charged tracks, the distance of the closest approach to the interaction point (IP) is required to be within 1 cm transversely and 3 cm along the e^+ beam. Photons are selected from neutral ECL clusters with an energy threshold $E_{\text{cluster}} > 0.1 \text{ GeV}$ and are separated by at least 30 cm from the extrapolated projection point of any charged track. The tracks and photons in an event are divided into two hemispheres in the e^+e^- center-of-mass system (CMS), with a plane

perpendicular to the thrust axis calculated from the momenta of all charged tracks and photons. We select 3-prong vs. 1-prong topology events, i.e. three charged tracks are in one hemisphere and one charged track in the other. We define the former hemisphere as the signal side and the latter as the tag side. The number of photons on the signal side should be less than or equal to two, to allow for photons from initial and final state radiation or photons radiated from electron tracks.

Electrons are identified by an electron likelihood that includes the dE/dx value measured with the CDC, the ratio of the cluster energy from the ECL to the track momentum measured with CDC, ACC hits and shower shape in ECL [14]. With this likelihood, electrons are selected with an average efficiency of 85% over the whole momentum range of those in the signal MC. The momentum of a charged track in the laboratory system p should be greater than 0.3 GeV/ c to avoid poorly identified electrons. In order to correct for the energy loss due to bremsstrahlung, the momentum of an electron track is recalculated adding the momentum of radiated photon clusters if an ECL cluster with energy less than 1.0 GeV is detected within a cone angle of 10° along the electron flight direction.

The muon likelihood is formed from two variables: the difference between the range calculated from the momentum of the particle and that measured with the KLM, as well as the χ^2 value of the KLM hits with respect to the extrapolated track [15]. The average efficiency is evaluated as 90% from signal MC for muon in the momentum range for LFV decays. For muons, p should be larger than 0.6 GeV/ c for the same reason as in the electron case.

Tracks that do not satisfy the requirements for electron or muon candidates are classified as hadrons. To distinguish kaons from pions, we use a likelihood ratio which is calculated from dE/dx , time-of-flight and the hits in the ACC. We achieve kaon efficiencies of 85% in the barrel and 80% in the endcap region. In these cases, p should be larger than 0.5 GeV/ c . The remaining tracks are treated as pions.

Vector mesons are reconstructed in the following decay modes: $\rho^0 \rightarrow \pi^+\pi^-$, $K^*(892)^0 \rightarrow K^+\pi^-$ and $\phi \rightarrow K^+K^-$. We calculate the vector meson mass, M_V . We then fit the M_V distribution of the signal MC with two Gaussian distributions to take into account the effects of the intrinsic width of the resonances and the detector resolution.

The width of the signal windows for each decay modes is $\pm 1.64\sigma$, where σ is the standard deviation of the broader Gaussian component: $445 \text{ MeV}/c^2 < M_\rho < 1092 \text{ MeV}/c^2$, $730 \text{ MeV}/c^2 < M_{K^*} < 1064 \text{ MeV}/c^2$ and $1005 \text{ MeV}/c^2 < M_\phi < 1035 \text{ MeV}/c^2$.

The background that remains after applying all the selection criteria based on

event topology and particle identification is dominated by Bhabha events. This background is effectively reduced by requiring the invariant masses calculated for all combinations of two oppositely charged tracks to be greater than $0.2 \text{ GeV}/c^2$, assuming the electron mass.

Backgrounds from $B\bar{B}$ and $c\bar{c}$ events are suppressed by the selection criteria listed above, however the background from $e^+e^- \rightarrow q\bar{q}$ continuum events with the light quarks u , d and s (uds continuum) is not negligible. Since these backgrounds often include π^0 decays, we require that the number of photons on the tag side n_γ not exceed 1. If the tag is an electron or muon, the n_γ requirement effectively suppresses the uds continuum background. For tags where the tag side is a pion, the selected events are investigated further as follows.

We measure the τ flight length l_τ using information on IP and τ vertex position that is reconstructed from the tracks on the signal side. Since τ leptons travel significant distance before decaying ($c\tau = 87\mu\text{m}$), this feature can be used to suppress background. Since τ -pair events have a more jet-like shape than uds continuum events and are distinguishable by use of shape variables. We use a normalized second Fox-Wolfram moment R_2 [16] to represent the event shape. Figure 1 shows the l_τ and R_2 distributions for τ -pair and uds continuum events. We calculate the two-dimensional probability density function (PDF) in the l_τ vs. R_2 plane, and form a likelihood ratio $\mathcal{L}_{\tau\tau}/(\mathcal{L}_{\tau\tau} + \mathcal{L}_{uds})$, where $\mathcal{L}_{\tau\tau}$ and \mathcal{L}_{uds} are the PDFs for τ -pair signal and uds continuum background, respectively. The condition $\mathcal{L}_{\tau\tau}/(\mathcal{L}_{\tau\tau} + \mathcal{L}_{uds}) > 0.45$ is optimized using MC. This condition removes 60% of uds continuum background, while 90% of the signal is kept when the track on the tag side is a pion. After combination of all selections including the n_γ and likelihood ratio requirements, the uds continuum background is suppressed by a factor of 10^5 .

We calculate the missing four-momentum for each event. In signal events, it is possible to reconstruct a τ mass from the missing momentum, 1-prong charged track momentum and all momenta of photons on the tag side, since there is no neutrino emission from the signal decays. Figure 2 shows the distributions of the τ mass on the tag side $M_{1\text{pr}}$ for the signal events and uds continuum background MC. There is a clear peak at the τ mass in the signal distribution, while the distribution for background process is smooth. Comparing the yield of these distributions, we optimize the central value and width of the signal windows independently for electron and muon modes: $0.85 \text{ GeV}/c^2 < M_{1\text{pr}} < 2.31 \text{ GeV}/c^2$ for the $\tau \rightarrow ehh$ and $\tau \rightarrow eV^0$ modes, and $1.06 \text{ GeV}/c^2 < M_{1\text{pr}} < 2.22 \text{ GeV}/c^2$ for the $\tau \rightarrow \mu hh$ and $\tau \rightarrow \mu V^0$ modes.

To identify signal τ decays, we reconstruct the invariant mass $M_{\ell hh}$ and CMS energy $E_{\ell hh}^*$ of selected events. We then calculate the energy difference $\Delta E^* \equiv E_{\ell hh}^* - E_{\text{beam}}^*$ and mass difference $\Delta M \equiv M_{\ell hh} - M_\tau$, where E_{beam}^* is the

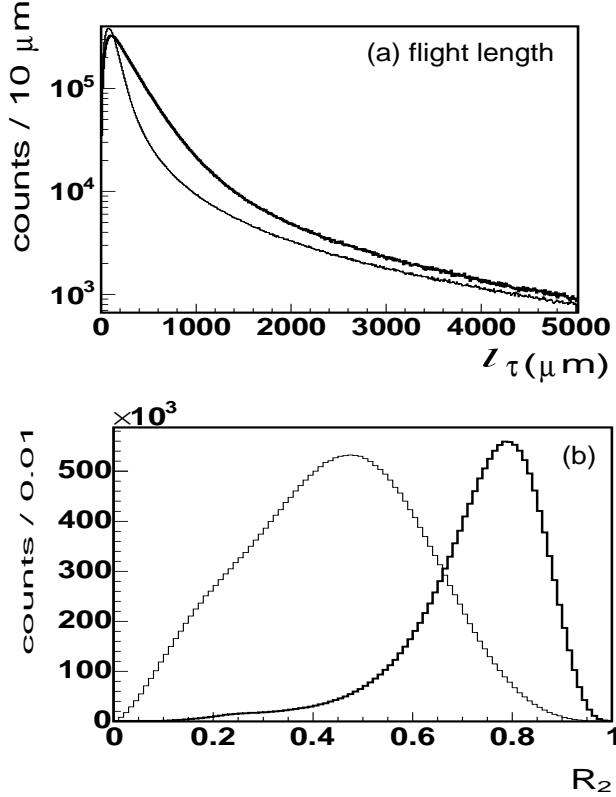


Fig. 1. (a) Flight length l_τ and (b) R_2 distributions of the signal MC events (thick line) and uds continuum events (thin line). The histogram normalization is arbitrary.

beam CMS energy and M_τ is the nominal τ mass. The signal events should have ΔE^* and ΔM around zero. We define the signal region in the ΔE^* - ΔM plane using the signal MC. Signal MC distributions have tails on the lower sides of ΔE^* and ΔM due to effects from initial and final state radiation, bremsstrahlung of electrons and ECL energy leakage. We consider signal MC events as properly reconstructed if they satisfy the conditions $-0.68 \text{ GeV} < \Delta E^* < 0.32 \text{ GeV}$ and $-0.25 \text{ GeV}/c^2 < \Delta M < 0.25 \text{ GeV}/c^2$. We thus define a rectangular signal region that contains 90% of properly reconstructed signal events. The boundaries of the signal region are summarized in Table 1.

3 Results

The signal MC events are generated assuming a uniform decay angular distribution of τ . Signal detection efficiencies ϵ , evaluated from the MC, are listed in the fourth column of Table 2 and vary from 2.68% to 5.30%. The actual decay angle distribution, however, depends on the model for the LFV interaction. In order to evaluate the possible effect of correlations, we examine $V - A$ and $V + A$ interactions using the formulae given in Ref. [17] and the relative

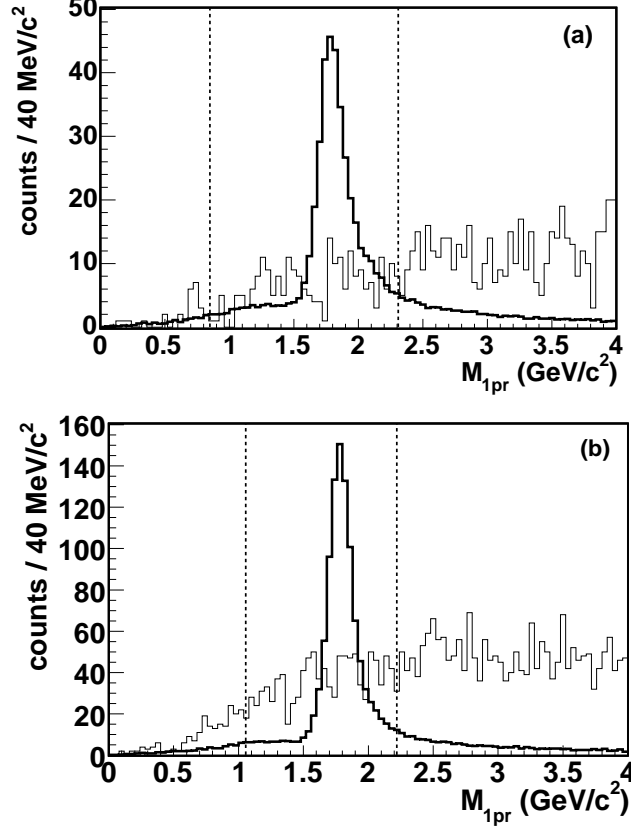


Fig. 2. M_{1pr} distributions for the signal (thick line) and uds continuum (thin line) MC events. The left figure (a) is for modes in which an electron is on the signal side, and the figure on the right (b) is for muon tags. Dashed lines show the boundaries of the signal region.

differences in the efficiencies from the uniform distribution ($\Delta\epsilon/\epsilon$) are taken as systematic errors of detection efficiencies.

After all selection requirements, some events remain in the signal region. From MC, we evaluate the number of background events from uds continuum and τ -pair production. We then scale to the data by the factor $\sigma\mathcal{L}_{\text{int}}/N_{\text{MC}}$, where σ is the cross section of this process, and N_{MC} is the number of generated events of the process. In the $\tau^- \rightarrow e^- h^+ h^-$ and $\tau^- \rightarrow e^- V^0$ modes, there is a contribution from two-photon $e^+e^- \rightarrow e^+e^-e^+e^-$, $e^+e^- \rightarrow e^+e^- \mu^+ \mu^-$, $e^+e^- \rightarrow e^+e^- u \bar{u}$, $e^+e^- \rightarrow e^+e^- d \bar{d}$ and $e^+e^- \rightarrow e^+e^- s \bar{s}$ processes. Since the equivalent luminosity for the MC simulation of two-photon processes is much smaller than \mathcal{L}_{int} , the contribution of the two-photon processes is estimated from a fit to the data in the ΔM sideband region, in which the contributions of uds continuum and τ -pair are fixed from MC and the two-photon shape is taken from MC with the normalization floated. For all modes the sideband region is $-0.5 \text{ GeV}/c^2 < \Delta M < 0.5 \text{ GeV}/c^2$, while the signal region $-96 \text{ MeV}/c^2 < \Delta M < 30 \text{ MeV}/c^2$ is blinded. The shape of the ΔM distribution is obtained after applying only the particle identification requirements.

Table 1

Definition of the signal regions for each decay mode.

Mode	ΔE^* (GeV)	ΔM (GeV/ c^2)
$\tau^- \rightarrow e^- \pi^+ \pi^-$	-0.10 - +0.04	-0.014 - +0.011
$\tau^- \rightarrow e^+ \pi^- \pi^-$	-0.09 - +0.04	-0.014 - +0.011
$\tau^- \rightarrow \mu^- \pi^+ \pi^-$	-0.07 - +0.03	-0.011 - +0.011
$\tau^- \rightarrow \mu^+ \pi^- \pi^-$	-0.07 - +0.03	-0.011 - +0.011
$\tau^- \rightarrow e^- \pi^+ K^-$	-0.10 - +0.04	-0.013 - +0.011
$\tau^- \rightarrow e^- \pi^- K^+$	-0.10 - +0.04	-0.012 - +0.010
$\tau^- \rightarrow e^+ \pi^- K^-$	-0.10 - +0.04	-0.014 - +0.010
$\tau^- \rightarrow e^- K^+ K^-$	-0.10 - +0.04	-0.010 - +0.008
$\tau^- \rightarrow e^+ K^- K^-$	-0.10 - +0.04	-0.013 - +0.009
$\tau^- \rightarrow \mu^- \pi^+ K^-$	-0.08 - +0.03	-0.009 - +0.009
$\tau^- \rightarrow \mu^- \pi^- K^+$	-0.07 - +0.03	-0.009 - +0.009
$\tau^- \rightarrow \mu^+ \pi^- K^-$	-0.08 - +0.03	-0.009 - +0.009
$\tau^- \rightarrow \mu^- K^+ K^-$	-0.07 - +0.03	-0.007 - +0.008
$\tau^- \rightarrow \mu^+ K^- K^-$	-0.07 - +0.03	-0.007 - +0.007
$\tau^- \rightarrow e^- \rho^0$	-0.10 - +0.04	-0.015 - +0.012
$\tau^- \rightarrow e^- K^*(892)^0$	-0.10 - +0.04	-0.013 - +0.011
$\tau^- \rightarrow e^- \bar{K}^*(892)^0$	-0.08 - +0.04	-0.012 - +0.010
$\tau^- \rightarrow e^- \phi$	-0.09 - +0.03	-0.010 - +0.008
$\tau^- \rightarrow \mu^- \rho^0$	-0.07 - +0.03	-0.011 - +0.011
$\tau^- \rightarrow \mu^- K^*(892)^0$	-0.08 - +0.03	-0.009 - +0.010
$\tau^- \rightarrow \mu^- \bar{K}^*(892)^0$	-0.08 - +0.03	-0.009 - +0.009
$\tau^- \rightarrow \mu^- \phi$	-0.08 - +0.03	-0.007 - +0.007

We verify that this shape does not change when additional selection criteria are applied by comparing the distribution before all selections and after each of them is successively imposed. It is known that K/π separation is different for data and MC. We measure identification efficiency and fake rate for both of them using calibration samples obtained from $D^* \rightarrow D^0[K^-\pi^+]\pi$ decays and apply a correction to the MC distributions. The ΔM distributions of data and expected background for the $\tau^- \rightarrow e^- \pi^+ \pi^-$ and $\tau^- \rightarrow \mu^- \pi^+ \pi^-$ modes after the corrections are shown in Figure 3. The number of expected background events in the signal region for each studied decay mode is given in the fifth column of Table 2. The uncertainty in the background expectation is dominated

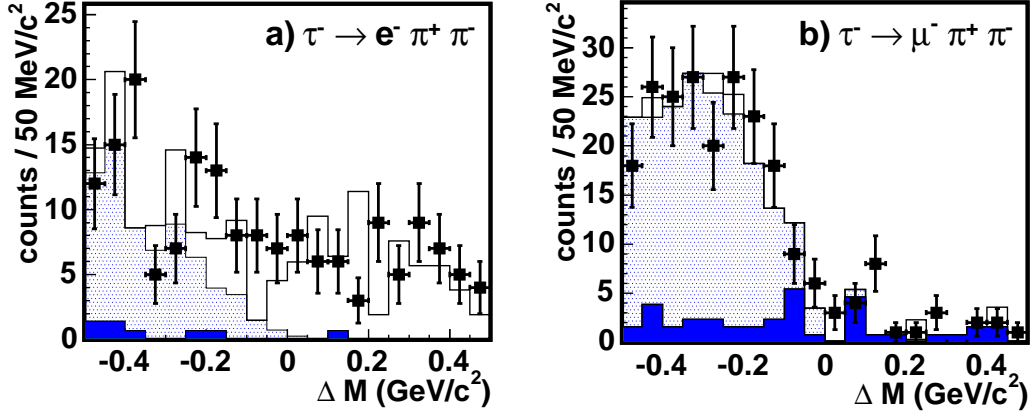


Fig. 3. ΔM distributions of experimental data (points with error bars) and expected background (histograms) for a) $\tau \rightarrow e^- \pi^+ \pi^-$ and b) $\tau \rightarrow \mu^- \pi^+ \pi^-$ modes after all selection criteria except for ΔM . Particle identification corrections (see text) have been applied to all MC distributions. Different patterns of the background histograms correspond to various kinds of the background: uds continuum (dark), τ -pair generic decays (shaded) and two-photon process (blank). MC histograms are cumulative and show general agreement between the data and MC.

by MC statistics.

The ΔE^* vs. ΔM plots for the experimental data for all decay modes are shown in Figure 4. The numbers of events observed in the signal regions are listed in the sixth column of Table 2. They are consistent with those expected from background distributions. We set the upper limits s_0 on the number of the signal events at 90% CL using the prescription of Feldman and Cousins [18]. The main systematic uncertainties on the detection efficiency come from track reconstruction (1.0% per track), electron identification (1.1% per electron), muon identification (5.4% per muon), kaon/pion separation (1.0% per kaon and pion), trigger efficiency (1.4%), statistics of the signal MC (1.0%) and uncertainties of the branching fractions of vector meson decays (1.2% for $\phi \rightarrow K^+ K^-$). The uncertainty on the number of τ -pair events mainly comes from the luminosity measurement (1.4%). The systematic uncertainties due to the angular distribution of LFV τ decays are summarized in the second column of Table 2, together with the total systematic errors $\Delta\epsilon/\epsilon$, which are used to evaluate the total errors of the sensitivities. To evaluate s_0 , we use the Poisson probability density function, which is convolved with the uncertainties on the sensitivities and expected background assuming the Gaussian shape [19,20].

Upper limits on the branching fractions \mathcal{B} are calculated as $\mathcal{B}(\tau \rightarrow \ell h h) < \frac{s_0}{2N_{\tau\tau}\epsilon\mathcal{B}_1}$ and $\mathcal{B}(\tau^- \rightarrow \ell V^0) < \frac{s_0}{2N_{\tau\tau}\epsilon\mathcal{B}_1\mathcal{B}_V}$, where $N_{\tau\tau}$ is the total number of the τ -pairs produced, \mathcal{B}_1 is the inclusive branching fraction for the 1-prong decay of τ and \mathcal{B}_V is the branching fraction of vector meson decay into charged

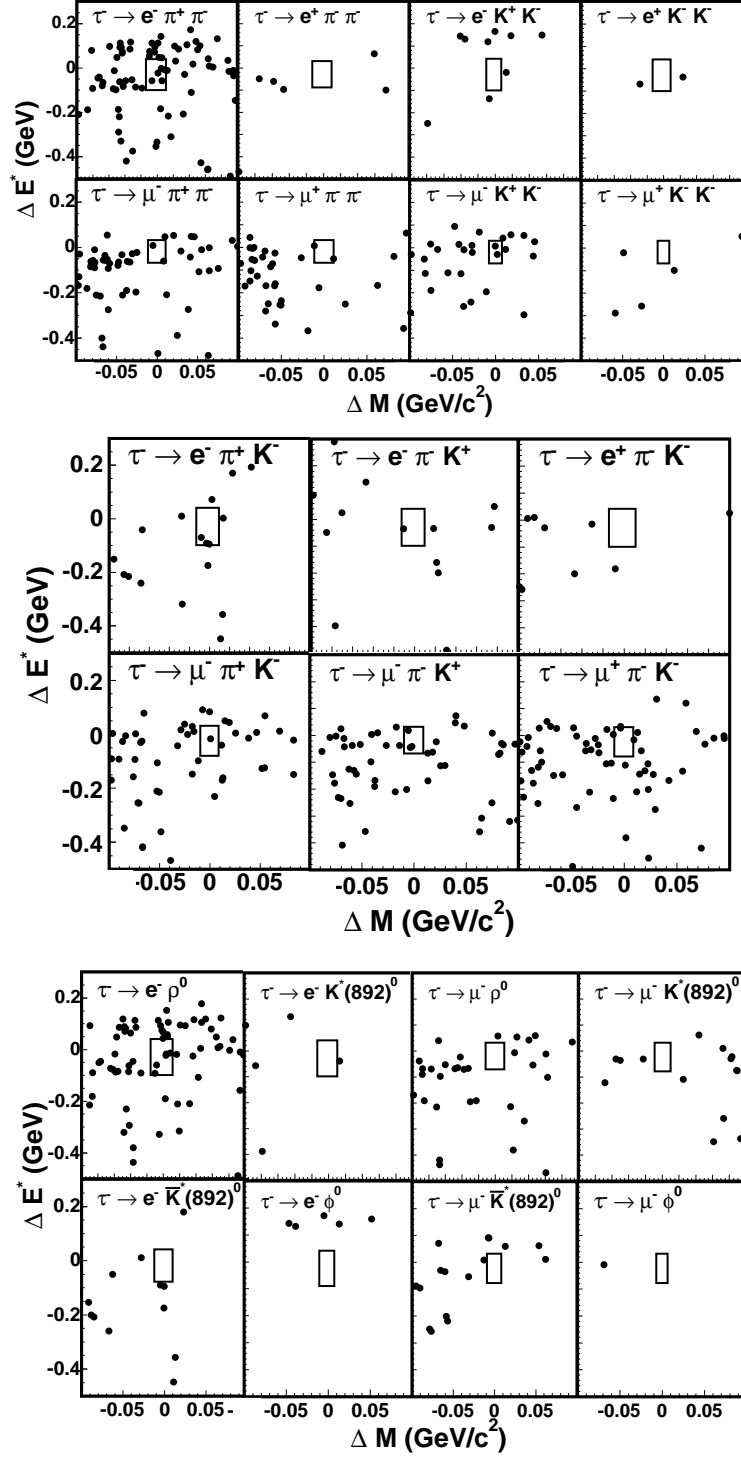


Fig. 4. ΔE^* vs. ΔM experimental data distribution after all selection criteria. The boundaries of the signal region are illustrated by solid boxes.

Table 2

Summary of detection efficiency ϵ and its systematic error $\Delta\epsilon/\epsilon$, background expectation, number of observed events and 90% C.L. upper limits on the branching fractions (BFs). For systematic uncertainty, LFV stands for the error due to the angular distribution of LFV decays, while “Total” combines LFV and all other errors.

Mode	$\Delta\epsilon/\epsilon$ (%)		Detection efficiency ϵ (%)	Expected background	Observed events	Upper limit on BF (90% CL)
	LFV	Total				
$\tau^- \rightarrow e^- \pi^+ \pi^-$	5.3	7.5	5.30	2.62 ± 1.07	6	7.3×10^{-7}
$\tau^- \rightarrow e^+ \pi^- \pi^-$	2.3	5.8	5.14	0.00 ± 0.26	1	2.0×10^{-7}
$\tau^- \rightarrow \mu^- \pi^+ \pi^-$	2.1	8.8	4.37	0.76 ± 0.26	2	4.8×10^{-7}
$\tau^- \rightarrow \mu^+ \pi^- \pi^-$	7.7	11.5	4.44	0.73 ± 0.30	1	3.4×10^{-7}
$\tau^- \rightarrow e^- \pi^+ K^-$	20.5	21.2	3.99	0.91 ± 0.25	3	7.2×10^{-7}
$\tau^- \rightarrow e^- \pi^- K^+$	17.4	18.2	4.11	1.27 ± 0.41	0	1.6×10^{-7}
$\tau^- \rightarrow e^+ \pi^- K^-$	12.8	13.9	4.03	0.74 ± 0.22	0	1.9×10^{-7}
$\tau^- \rightarrow e^- K^- K^+$	21.9	22.5	3.12	0.34 ± 0.20	0	3.0×10^{-7}
$\tau^- \rightarrow e^+ K^- K^-$	5.4	7.6	3.06	0.09 ± 0.07	0	3.1×10^{-7}
$\tau^- \rightarrow \mu^- \pi^+ K^-$	15.8	18.0	3.43	2.35 ± 0.44	1	2.7×10^{-7}
$\tau^- \rightarrow \mu^- \pi^- K^+$	19.1	20.9	3.32	1.85 ± 0.32	3	7.3×10^{-7}
$\tau^- \rightarrow \mu^+ \pi^- K^-$	25.4	26.8	3.53	2.53 ± 0.38	1	2.9×10^{-7}
$\tau^- \rightarrow \mu^- K^- K^+$	8.7	12.2	2.76	0.48 ± 0.19	2	8.0×10^{-7}
$\tau^- \rightarrow \mu^+ K^- K^-$	38.2	39.2	2.70	0.09 ± 0.06	0	4.4×10^{-7}
$\tau^- \rightarrow e^- \rho^0$	5.3	7.5	5.03	2.55 ± 1.04	5	6.5×10^{-7}
$\tau^- \rightarrow e^- K^*(892)^0$	17.4	18.2	4.12	0.76 ± 0.34	0	3.0×10^{-7}
$\tau^- \rightarrow e^- \bar{K}^*(892)^0$	20.5	21.2	3.68	0.16 ± 0.10	0	4.0×10^{-7}
$\tau^- \rightarrow e^- \phi$	21.9	22.5	2.94	0.04 ± 0.04	0	7.3×10^{-7}
$\tau^- \rightarrow \mu^- \rho^0$	2.1	8.8	4.40	0.26 ± 0.12	0	2.0×10^{-7}
$\tau^- \rightarrow \mu^- K^*(892)^0$	19.1	20.9	3.61	0.37 ± 0.14	0	3.9×10^{-7}
$\tau^- \rightarrow \mu^- \bar{K}^*(892)^0$	15.8	18.0	3.42	0.49 ± 0.19	0	4.0×10^{-7}
$\tau^- \rightarrow \mu^- \phi$	8.7	12.2	2.68	0.00 ± 0.18	0	7.7×10^{-7}

hadrons. We use $\mathcal{B}_1 = (85.35 \pm 0.07)\%$ and $\mathcal{B}_\phi = (49.2 \pm 0.6)\%$ from the 2005 web update of Ref. [13]. The resulting upper limits on the branching fractions are summarized in the last column of Table 2.

4 Discussion

Our final results for 90% upper limits on the branching fractions for the $\tau \rightarrow \ell hh$ modes, shown in Table 2, are in the range $(1.6 - 8.0) \times 10^{-7}$. Our results for $\tau \rightarrow \ell hh$ and $\tau \rightarrow \ell V^0$ modes are one order of magnitude more restrictive than those obtained in the CLEO experiment [4] except for a few decay modes. The results for $\tau^- \rightarrow \ell hh$ modes are comparable to those from BaBar [5].

While in many extensions of the Standard Model the predicted values of the branching fractions of LFV decays are very small and out of reach for current experiments, some models allow enhancements of such decays to a level very close to the experimentally accessible range at the B factories. For example, detailed analysis of various LFV τ lepton decays in the framework of MSSM show that at small $\tan\beta$ and appropriate values of other model parameters the branching ratio of the $\tau^- \rightarrow \mu^- \rho^0$ decay can be as high as 10^{-8} [21].

The improved sensitivity to rare τ lepton decays achieved in this work can be used to constrain the parameters of models with heavy Dirac neutrinos [3]. In this model the expected branching fractions of various LFV decays are evaluated in terms of combinations of the model parameters. These combinations, denoted $y_{\tau e}^2$ and $y_{\tau \mu}^2$ for τ decays involving an electron and a muon, respectively, can vary from 0 to 1. Our best 90% upper limit for the modes with an electron, $y_{\tau e}^2 < 0.24$, can be set from the $\tau^- \rightarrow e^- \rho^0$ decay. The best corresponding limit for modes with a muon studied in this work is set from the $\tau^- \rightarrow \mu^- \rho^0$ mode, $y_{\tau \mu}^2 < 0.38$. This bound is more restrictive than any other limits set on LFV decays of the τ .

Our results can also be used to constrain energy scale of new physics in models with dimension-six effective fermionic operators that induce $\tau - \mu$ mixing [22]. From our upper limits for the branching fractions of $\tau^- \rightarrow \mu^- \rho^0$, $\tau^- \rightarrow \mu^- \phi$ and $\tau^- \rightarrow \mu^- K^*(892)^0$ the bounds $\Lambda_{uu,dd} > 29.4$ TeV, $\Lambda_{ss} > 24.8$ TeV and $\Lambda_{ds} > 26.8$ TeV, respectively, can be obtained for the models with vector operators.

5 Summary

We have searched for LFV decays $\tau \rightarrow \ell hh$ and $\tau \rightarrow \ell V^0$ using a 158.0 fb^{-1} (140.9×10^6 τ -pair events) data sample in the Belle experiment. No evidence for a signal of these decay modes is observed and upper limits on the branching fractions are set in the range $(1.6 - 8.0) \times 10^{-7}$, which are one order of magnitude more restrictive than those previously obtained by the CLEO experiment. For $\tau \rightarrow \ell hh$ modes, the results are comparable to recent limits

from BaBar [5].

We thank the KEKB group for the excellent operation of the accelerator, the KEK cryogenics group for the efficient operation of the solenoid, and the KEK computer group and the National Institute of Informatics for valuable computing and Super-SINET network support. We acknowledge support from the Ministry of Education, Culture, Sports, Science, and Technology of Japan and the Japan Society for the Promotion of Science; the Australian Research Council and the Australian Department of Education, Science and Training; the National Science Foundation of China and the Knowledge Innovation Program of Chinese Academy of Sciences under contract No. 10575109 and IHEP-U-503; the Department of Science and Technology of India; the BK21 program of the Ministry of Education of Korea, and the CHEP SRC program and Basic Research program (grant No. R01-2005-000-10089-0) of the Korea Science and Engineering Foundation; the Polish State Committee for Scientific Research under contract No. 2P03B 01324; the Ministry of Science and Technology of the Russian Federation; the Slovenian Research Agency; the Swiss National Science Foundation; the National Science Council and the Ministry of Education of Taiwan; and the U.S. Department of Energy.

References

- [1] W.J. Marciano and A.I. Sanda, Phys. Lett. B **67**, 303 (1977); B.W. Lee and R.E. Shrock, Phys. Rev. D **16**, 1444 (1977); T.P. Cheng and L.F. Li, Phys. Rev. D **16**, 1425 (1977).
- [2] A. Ilakovac, Phys. Rev. D **54**, 5653 (1996).
- [3] A. Ilakovac, Phys. Rev. D **62**, 036010 (2000).
- [4] D.W. Bliss *et al.* (CLEO Collaboration), Phys. Rev. D **57**, 5903 (1998).
- [5] B.Aubert *et al.* (BaBar Collaboration), Phys. Rev. Lett. **95**, 191801 (2005).
- [6] A. Abashian *et al.* (Belle Collaboration), Nucl. Instr. and Meth. A **479**, 117 (2002).
- [7] S. Kurokawa and E. Kikutani, Nucl. Instr. and Meth. A **499**, 1 (2003), and other papers included in this Volume.
- [8] KORALB(v2.4)/TAUOLA(v2.6); S. Jadach and Z. Was, Comp. Phys. Commun. **85**, 453 (1995); *ibid*, **64**, 267 (1991); S. Jadach, Z.Was, R. Decker, and J.H.Kühn, Comp. Phys. Commun. **76**, 361 (1993); *ibid*, **70**, 69 (1992); *ibid*, **64**, 275 (1991); E. Barberio and Z. Was, Comp. Phys. Commun. **64**, 275 (1990).
- [9] S. Jadach, B.F.L. Ward, Z. Was, Comp. Phys. Commun. **130** 260 (2000).

- [10] R. Brun *et al.*, GEANT 3.21, CERN Report DD/EE/84-1, 1984.
- [11] see <http://www.lns.cornell.edu/public/CLEO/soft/qq>.
- [12] F.A. Berends, P.H. Daverveldt, and R. Kleiss, Comp. Phys. Commun. **40**, 285 (1986).
- [13] S. Eidelman *et al.* (Particle Data Group), Phys. Lett. B **592**, 1 (2004).
- [14] K. Hanagaki *et al.*, Nucl. Instr. and Meth. A **485**, 490 (2002).
- [15] A. Abashian *et al.*, Nucl. Instr. and Meth. A **491**, 69 (2002).
- [16] G. C. Fox and S. Wolfram, Phys. Rev. Lett. **41**, 1581 (1978).
- [17] R. Kitano and Y. Okada, Phys. Rev. D **63**, 113003 (2001).
- [18] G.J. Feldman and R.D. Cousins, Phys. Rev. D **57**, 3873 (1998).
- [19] R.D. Cousins and V.L Highland, Nucl. Instr. and Meth. A **320**, 331 (1992) .
- [20] J. Conrad, O. Botner, A. Hallgren and Carlos P. de los Heros, Phys. Rev. D **67**, 012002 (2003).
- [21] A. Brignole and A. Rossi, Nucl. Phys. B **701**, 3 (2004).
- [22] D. Black et al., Phys. Rev. D **66**, 053002 (2002).